

## Optical functions of $\text{BiI}_3$ as measured by generalized ellipsometry

G. E. Jellison, Jr., J. O. Ramey, and L. A. Boatner

*Solid State Division, Oak Ridge National Laboratory, Oak Ridge, Tennessee 37831*

(Received 16 November 1998)

The optical functions of  $\text{BiI}_3$  have been measured using two-modulator generalized ellipsometry (2-MGE). The measurements were made on crystals grown by a vapor-transport method under conditions that produced relatively thick ( $\sim 1$  mm) single crystals whose growth habits were characterized by the development of large faces for orientations other than that of the basal plane (i.e., other than the plane perpendicular to the  $\mathbf{c}$  axis of the  $\text{BiI}_3$  rhombohedral structure.) By performing 2-MGE measurements on crystal faces other than the basal plane, it is possible to determine both the ordinary and extraordinary dielectric functions of the material. While the ordinary dielectric functions have been determined from previous normal-incidence reflectivity measurements, to our knowledge the extraordinary dielectric functions obtained here using the 2-MGE method are new results. Both the ordinary and extraordinary band edges are the same energy (1.99 eV), and both exhibit a strong exciton. The matrix element for the ordinary transition, however, is a factor of 6 to 10 larger than the matrix element for the extraordinary transition near the band edge. [S0163-1829(99)03116-1]

### INTRODUCTION

Bismuth Iodide ( $\text{BiI}_3$ ) is a layered semiconductor with a band gap of  $\sim 2$  eV. Due to its strong intrinsic optical anisotropy, considerable prior interest has been exhibited in the optical properties of this material. In addition, the relatively large band gap and the heavy atoms comprising  $\text{BiI}_3$  have made it a candidate material for development as a room-temperature gamma-ray detector.

The crystal structure of bismuth tri-iodide ( $\text{BiI}_3$ ) is rhombohedral, making it optically uniaxial with the  $c$  axis perpendicular to the basal plane. Each bismuth atom is octahedrally coordinated with six iodine atoms, and each structural layer consists of the three atomic layers I-B-I. The structural layers are weakly bonded by van der Waals forces, making this a distinct cleavage plane. From a planar perspective along the  $c$  axis, only two-thirds of the possible bismuth sites are occupied, giving three possible orientations of the unoccupied site. Moreover, since the interlayer bonding is so weak, stacking faults represent the most common defects found in these crystals. Since the  $\text{BiI}_3$  crystal has sixfold symmetry, it is optically uniaxial, and requires two dielectric functions (ordinary, for light polarized perpendicular to the optic axis  $\mathbf{E} \perp \mathbf{c}$ , and extraordinary, for light polarized parallel to the optic axis  $\mathbf{E} \parallel \mathbf{c}$ ).

Single crystals of  $\text{BiI}_3$  have previously been grown using both the physical-vapor-transport method<sup>1-3</sup> or the vertical Bridgman technique.<sup>4</sup> Thus far, crystals exhibiting the highest structural quality and the highest purity have been produced by means of the vapor-transport approach. Usually,  $\text{BiI}_3$  crystals grown by vapor-transport methods exhibit a platelet morphology. Nason and Keller<sup>3</sup> have reported the vapor-transport growth of a 2.6-gm  $\text{BiI}_3$  crystal having dimensions of  $1.2 \times 1.2 \times 0.4 \text{ cm}^3$  and exhibiting several well-developed growth faces. The largest growth face was the (0001) basal plane, but the (1120) and (1123) faces, as well as their symmetric counterpart planes, were also of significant size. Bismuth tri-iodide has also been grown in the form of polycrystalline thin films with the  $\mathbf{c}$  axis oriented perpen-

dicular to the growth surface.<sup>5</sup>

Most of the previous optical characterization of  $\text{BiI}_3$  has been performed by means of optical transmission, optical reflection, and photoluminescence measurements made using crystals that were cleaved along the (0001) basal plane so that the optical axis of the material was perpendicular to the sample surface.<sup>6-11</sup> In these cases, when the incident light was at near-normal incidence, the measurements were only sensitive to the ordinary complex refractive index of the material. Using reflectivity, Komatsu and Kaifu<sup>5</sup> observed a strong exciton at the band gap ( $\sim 2.0$  eV), and they reported a strongly dispersive refractive index below the band gap of thin-film  $\text{BiI}_3$ . Several features could be observed in the reflectivity spectra that represent critical points in the Brillouin zone as calculated by pseudopotential techniques.<sup>12</sup>

Below the band gap, Kaifu and Komatsu<sup>7</sup> used temperature-dependent optical absorption measurements, which showed a strong Urbach-tail absorption below the direct band gap at higher temperatures, and at lower temperatures, both an indirect transition (2.008 eV) and a direct transition (2.080 eV). In the energy region from  $\sim 1.985$  to  $\sim 2.008$  eV, several sharp transitions were observed at low temperatures both in the optical absorption and in photoluminescence results that were attributed to stacking-fault defects in the material.<sup>9-11</sup>

### EXPERIMENT

In the present paper, we describe the results of two-modulator generalized ellipsometry (2-MGE) measurements made using single crystals of  $\text{BiI}_3$  grown by the physical-vapor-transport technique. The 2-MGE method<sup>13</sup> has previously been established as an accurate approach to measuring the optical functions of materials such as  $\text{TiO}_2$  (Ref. 14) and  $\text{ZnO}$  (Ref. 15)—particularly above the optical band gap. If the sample geometry is such that the optical axis of a uniaxial crystal such as  $\text{BiI}_3$  is significantly off normal, then it is possible to determine both the ordinary and extraordinary dielectric functions by means of a single measurement.

The 2-MGE technique and apparatus have previously been described in some detail.<sup>3</sup> Briefly, the 2-MGE consists of two photoelastic modulator/polarizer pairs—one pair acting as the polarization-state generator (PSG), and the other acting as the polarization-state detector (PSD). Each modulator operates at a different resonant frequency (50.2 and 60.3 kHz in our case), making it possible to measure eight different elements of the reduced Mueller matrix. For certain orientations of the PSG and the PSD (for example,  $\theta_{\text{PSG}} = 0^\circ$  and  $\theta_{\text{PSD}} = 45^\circ$  or  $\theta_{\text{PSG}} = 45^\circ$  and  $\theta_{\text{PSD}} = 0^\circ$ ), the eight elements of the reduced Mueller matrix can be transformed to the six elements of the complex reduced Jones matrix, i.e., to the form:

$$\mathbf{J} = \begin{pmatrix} \rho_{\text{pp}} & \rho_{\text{ps}} \\ \rho_{\text{sp}} & 1 \end{pmatrix}, \quad (1)$$

where  $\rho_{xy} = r_{xy}/r_{ss}$ ,  $x, y = s, p$ . The complex reflection coefficients are given by  $r_{\text{pp}}$ ,  $r_{\text{ss}}$ ,  $r_{\text{sp}}$ , and  $r_{\text{ps}}$ , where  $r_{\text{sp}}$  and  $r_{\text{ps}}$  are the cross-polarization reflection coefficients. The quantities  $r_{\text{sp}}$  and  $r_{\text{ps}}$  are 0 if the material is isotropic or if the optical axis is either in the plane of incidence or perpendicular to the plane of incidence.

The  $\text{BiI}_3$  samples employed in the present studies were vapor-transport-produced single-crystal platelets that were grown in sealed, evacuated dual-chamber quartz ampoules. The  $\text{BiI}_3$  compound was initially synthesized in the first chamber of the ampoule by reacting stoichiometric amounts of high-purity anhydrous iodine and high-purity bismuth metal. The two chambers of the synthesis/growth ampoule were separated by a quartz frit, which prevented the physical transport of contaminants from the synthesis chamber into the growth chamber. The ampoule was positioned in a tube furnace so that the second chamber (i.e., the chamber that had not been utilized for the  $\text{BiI}_3$  synthesis from the elemental components) was located in a region that was cooler relative to that of the chamber containing the synthesized  $\text{BiI}_3$ . Vapor transport of the synthesized growth charge was temperature induced, and the resulting single crystals nucleated and grew in the area near the cooler pointed tip of the second chamber. Higher-purity  $\text{BiI}_3$  single crystals were produced by harvesting most of the vapor-transport-grown crystals from the second (growth) chamber and then loading these crystals into the first chamber of a new ampoule. New vapor-transport crystals could then be grown in the second chamber of the new ampoule starting with vapor-transport-grown material as the feed material in place of initially synthesized  $\text{BiI}_3$ . In some cases, this sequential harvesting and reloading/growth process was repeated three to five times. Since there is some loss of material and since the transport is not always complete, the total yield and crystal size after several sequential vapor-transport-growth runs is generally relatively small, and therefore, the  $\text{BiI}_3$  crystals employed in the present paper were nominally transported two to three times.

The resulting  $\text{BiI}_3$  single crystals all had a well-developed (0001) basal-plane face, and some crystals also had reasonably large  $\{hkz1\}$  and  $\{hkz2\}$  faces, where  $z = -h - k$ . The optical axis of the crystal was, therefore, perpendicular to the (0001) face ( $\theta = 0^\circ$ ), but  $\theta = 72.6^\circ$  off normal for the  $\{hkz1\}$  face and  $\theta = 57.8^\circ$  for the  $\{hkz2\}$  face. Two crystals were selected from a growth ampoule that exhibited large

$\{hkz1\}$  and  $\{hkz2\}$  faces so that the ellipsometry measurements could be carried out using a sample surface where the optical axis was significantly off normal. Several 2-MGE measurements were made at an angle of incidence of  $64.77^\circ$  on the samples selected, including measurements off the  $\{hkz1\}$ ,  $\{hkz2\}$ , and (0001) faces, and at several azimuthal orientations of the optical axis with respect to the plane of incidence ( $\varphi = 0^\circ, 45^\circ, 90^\circ$ , and  $135^\circ$ ). Since the  $\{hkz1\}$  and the  $\{hkz2\}$  faces were both small, focusing lenses were used to reduce the spot size on the crystal to  $\sim 0.5 \times 2.0$  mm. The residual strain in the lenses was measured, and the resulting 2-MGE data were corrected for the strain-induced birefringence of the lenses.

## RESULTS AND DISCUSSION

Separate determinations of the ordinary and the extraordinary optical functions could be made from measurements using the  $\{hkz1\}$  and the  $\{hkz2\}$  faces, and at azimuthal angles of  $\varphi = 45^\circ$  and  $135^\circ$  with respect to the plane of incidence. The surface roughness was determined using a procedure similar to that described in Ref. 15. The data below the direct band edge ( $\sim 2.0$  eV or 620 nm) was fit to a two-layer model consisting of surface roughness over  $\text{BiI}_3$ . The optical functions of the surface-roughness layer were approximated using an isotropic Bruggeman effective medium consisting of  $\sim 50\%$  voids and  $\sim 50\%$   $\text{BiI}_3$ , where the optical functions were taken to be the average of the ordinary and extraordinary optical functions. The ordinary and extraordinary optical functions of  $\text{BiI}_3$  in this region were parameterized using the Lorentz approximation. The resulting void fraction was 0.5 within the error limits, and the surface-roughness thickness was 5 to 8 nm. The complex dielectric function of  $\text{BiI}_3$  was then determined by mathematically removing the surface roughness as described in Refs. 14 and 15. Figures 1 and 2 show the average dielectric functions representing six separate determinations, where the complex dielectric function is given by

$$\varepsilon = \varepsilon_1 + i\varepsilon_2 = \tilde{n}^2 = (n + ik)^2, \quad (2)$$

the absorption coefficient by

$$\alpha = 4\pi k/\lambda, \quad (3)$$

and the normal incidence reflectivity by

$$R = \frac{(n-1)^2 + k^2}{(n+1)^2 + k^2}. \quad (4)$$

Figure 3 shows the absorption coefficient for the ordinary absorption coefficient determined using ellipsometry and optical-transmission measurements.

Many features of the ordinary spectra ( $\mathbf{E} \perp \mathbf{c}$ ) have been previously identified from normal-incidence reflection and transmission measurements. The calculated reflectivity shown in Fig. 2 agrees substantially with the room-temperature reflectivity measurements of Komatsu and Kaifu.<sup>6</sup> The long tail below  $\sim 1.9$  eV is an exciton-phonon Urbach tail, where

$$\alpha(E) = \alpha_0 \exp[-\sigma(E_0 - E)/kT]. \quad (5)$$

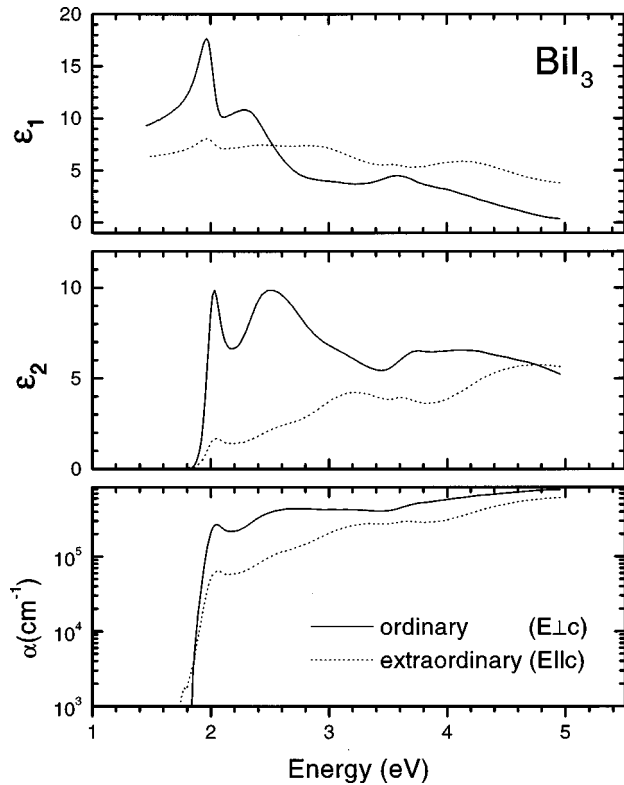


FIG. 1. The real and imaginary parts of the dielectric function ( $\epsilon_1$  and  $\epsilon_2$ ) as well as the absorption coefficient  $\alpha$  for bismuth iodide ( $\text{BiI}_3$ ). The ordinary dielectric function and absorption coefficient are shown by solid lines, and the extraordinary dielectric function and absorption coefficient are shown by the dotted lines.

The data from the transmission results shown in Figure 3 yield  $\sigma = 1.01$  (as shown by the straight line), which agrees with the results obtained by Kaifu and Komatsu.<sup>7</sup> The first peak in  $\epsilon_2$  near 2 eV is due to an exciton associated with the direct absorption edge.<sup>5</sup> According to the pseudopotential calculations of Schlüter *et al.*,<sup>12</sup> the energy gap in  $\text{BiI}_3$  is a direct gap at the  $A$  point in the Brillouin zone. The broad feature near 2.5 eV in the optical spectrum is tentatively assigned to transitions on the  $L$ - $U$ - $M$  line in the Brillouin zone. The feature near 3.6 eV is excitonic, but cannot be associated with a critical point in the Brillouin zone from the band structure of Ref. 12. Below the direct band gap  $\epsilon_2 = 0$  and  $\epsilon_1$  (or equivalently  $n$ ) is highly dispersive. As expected, the value of  $n$  obtained in this paper for solid  $\text{BiI}_3$  is somewhat higher than that obtained by Komatsu and Kaifu<sup>5</sup> for thin-film  $\text{BiI}_3$  (i.e., at 800 nm,  $n = 3.13$  for bulk  $\text{BiI}_3$  and  $n = 3.00$  for thin-film  $\text{BiI}_3$ ).

The extraordinary dielectric functions for  $\text{BiI}_3$  are new to this paper and are shown by the dotted lines in Figs. 1 and 2. Clearly, near the band edge  $\epsilon_{2o} > \epsilon_{2e}$  (at the excitonic peak at 2.03 eV,  $\epsilon_{2o} = 9.74$  while  $\epsilon_{2e} = 1.67$ , a ratio of 5.8:1) indicating that the matrix elements for light polarized along the optical axis are considerably smaller than for light polarized perpendicular to the optical axis; this contradicts the statement made in Ref. 12 that  $\epsilon_{2o} < \epsilon_{2e}$ . A similar observation can be made from the ordinary and extraordinary dielectric-function spectra of mercuric iodide.<sup>16</sup> However, the extraordinary band edge is very nearly the same energy as the energy of the ordinary band edge, and an exciton is also

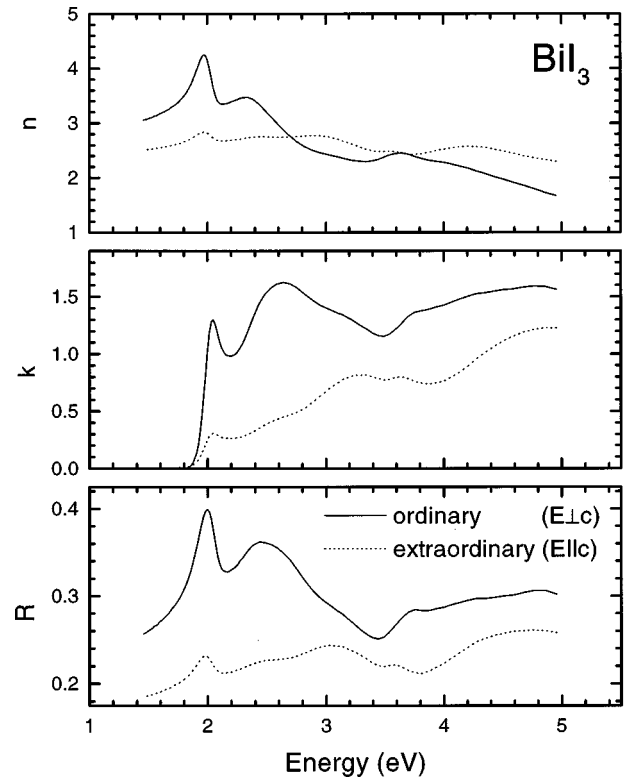


FIG. 2. The real and imaginary parts of the refractive index ( $n$  and  $k$ ) as well as the normal-incidence reflectivity  $R$  for bismuth iodide ( $\text{BiI}_3$ ). The ordinary refractive index and reflectivity are shown by solid lines, and the extraordinary refractive index and reflectivity are shown by the dotted lines.

associated with the extraordinary band edge. Since it was not possible to obtain very thin transmission samples where the optical axis is in the surface plane of the sample, it was not possible to repeat the transmission measurements shown in Fig. 3 for the extraordinary absorption coefficient. The large feature at 2.5 eV in the ordinary spectrum is not repeated in

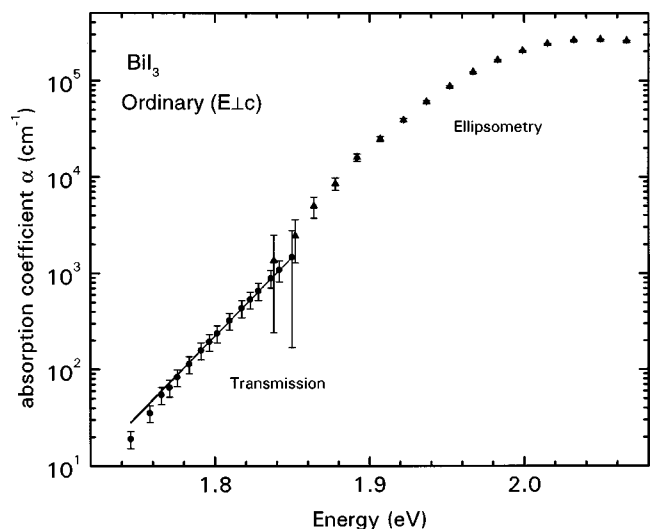


FIG. 3. The ordinary absorption coefficient of  $\text{BiI}_3$  near the band edge as determined by ellipsometry and transmission. The solid line through the transmission data represents a fit of the transmission data to Urbach's rule [see Eq. (5)].

TABLE I. The results of the fit to the excitonic features in the real and imaginary parts of the dielectric function near the band edge of BiI<sub>3</sub>.

Parameter	Ordinary ( $\mathbf{E} \perp \mathbf{c}$ )	Extraordinary ( $\mathbf{E} \parallel \mathbf{c}$ )
Band edge $E_g$ (eV)	$1.991 \pm 0.005$	$1.997 \pm 0.0021$
Excitation energy $R$ (eV)	$0.009 \pm 0.001$	$0.017 \pm 0.005$
Band broadening parameter $\Gamma_0$ (eV)	$0.019 \pm 0.003$	$0.021 \pm 0.006$
Exciton broadening parameter $\Gamma_{\text{ex}}$ (eV)	$0.047 \pm 0.008$	$0.037 \pm 0.014$
Amplitude $A$	$168 \pm 17$	$15 \pm 2$
$\chi^2$	10.8	4.5

the extraordinary spectrum, indicating that the transition associated with it is selection-rule limited. The exciton-related inflection at 3.6 eV is also observed in the extraordinary spectrum.

To further understand the excitonic feature near the band gap, the real and imaginary parts of the dielectric function near the band edge were fit to the theoretical formulation of Holden *et al.*<sup>17</sup> for an exciton at a two-dimensional direct band edge. The results are summarized in Table I. The  $\chi^2$  for both fits is quite large, indicating that the model does not fit the data within the error limits of the data; this was also noted for the excitonic features in ZnO as discussed in Ref. 15 and is due in part to the Lorentzian-broadening assumption of the excitonic features in Ref. 17. However, certain observations can be made concerning the results shown in Table I. First, the band energies  $E_g$ , the band-broadening parameter  $\Gamma_0$ , and the exciton-broadening parameter  $\Gamma_{\text{ex}}$  are essentially the same for both the ordinary and extraordinary

dielectric functions within the error limits. Second, the excitonic energy  $R$  is somewhat smaller for the ordinary dielectric function than for the extraordinary dielectric function, although this could also be due in part to the poor fit of the model to the data. Finally, the amplitude  $A$  (which is proportional to the matrix element for the optical transition) is about a factor of 10 larger for the ordinary dielectric function than for the extraordinary dielectric function.

#### ACKNOWLEDGMENTS

The authors would like to acknowledge F. A. Modine for carefully reading this paper and D. P. Corrigan for his assistance. This research was sponsored by the Division of Materials Science, U.S. Department of Energy under Contract No. DE-AC05-96OR22464 with Lockheed Martin Energy Research Corp.

<sup>1</sup>B. J. Curtis and H. R. Brunner, Mater. Res. Bull. **9**, 715 (1974).

<sup>2</sup>M. Schieber, T. J. Davies, W. F. Schnepfle, P. T. Randtke, and R. C. Carlston, J. Appl. Phys. **45**, 5371 (1974).

<sup>3</sup>D. Nason and L. Keller, J. Cryst. Growth **156**, 221 (1995).

<sup>4</sup>M. A. George, K.-T. Chen, W. E. Collins, A. Burger, D. Nason, and L. A. Boatner, J. Vac. Sci. Technol. B **14**, 1096 (1996).

<sup>5</sup>T. Komatsu and Y. Kaifu, J. Phys. Soc. Jpn. **40**, 1062 (1976).

<sup>6</sup>E. F. Gross, V. I. Perel', and R. I. Shekhammet'ev, Pis'ma Zh. Eksp. Teor. Fiz. **13**, 320 (1971) [JETP Lett. **13**, 229 (1971)].

<sup>7</sup>Y. Kaifu and T. Komatsu, J. Phys. Soc. Jpn. **40**, 1377 (1976).

<sup>8</sup>V. M. Shmandii, V. K. Miloslavskii, and V. V. Mussil, Fiz. Tverd. Tela (Leningrad) **21**, 2409 (1979) [Sov. Phys. Solid State **21**, 1386 (1979)].

<sup>9</sup>K. Watanabe, T. Karasawa, T. Komatsu, and Y. Kaifu, J. Phys. Soc. Jpn. **55**, 897 (1986).

<sup>10</sup>Y. Kaifu, J. Lumin. **42**, 61 (1988).

<sup>11</sup>T. Komatsu, T. Iika, I. Akai, T. Aikami, and V. F. Agekyan, Fiz. Tverd. Tela. (St. Petersburg) **37**, 2433 (1995) [Phys. Solid State **37**, 1332 (1995)].

<sup>12</sup>M. Schlüter, M. L. Cohen, S. E. Kohn, and C. Y. Fono, Phys. Status Solidi B **78**, 737 (1976).

<sup>13</sup>G. E. Jellison, Jr. and F. A. Modine, Appl. Opt. **36**, 8184 (1997); **36**, 8190 (1997).

<sup>14</sup>G. E. Jellison, Jr., F. A. Modine, and L. A. Boatner, Opt. Lett. **22**, 1808 (1997).

<sup>15</sup>G. E. Jellison, Jr. and L. A. Boatner, Phys. Rev. B **58**, 3586 (1998).

<sup>16</sup>H. Yao, B. Johs, and R. B. James, Phys. Rev. B **56**, 9414 (1997).

<sup>17</sup>T. Holden, P. Ram, F. H. Pollak, J. L. Freeouf, B. X. Yang, and M. C. Tamargo, Phys. Rev. B **56**, 4037 (1997).